operators are in direct voice communication, their measurements are performed on the same burst. T_0 will vary from burst to burst, while δ remains constant for numerous paths if the frequency standards at each terminal are maintained at sufficient accuracy. The difference between the two readings is $(T_0+\delta)-(T_0-\delta)$ or 2δ. Therefore, the resolver at Station 2 is adjusted by an amount equal to δ, so that the transmitters will then be driven in synchronism.

This method of instantaneous time synchronization is unique in that the actual propagation time is measured, which eliminates the calculations required in Loran-C. There are several reasons, however, why this technique is not used in an HF time synchronization system: 1) multipath phenomena prevent the leading edge of a pulse from being resolved to better than a few hundred microseconds; 2) the ionosphere exhibits considerable phase instability in the HF region of the spectrum, and 3) the allowable bandwidths are rather narrow. These factors, then, eliminate using HF for a very accurate phase detection system for time synchronization. Skywave interference is another limiting condition. The meteor-burst propagation mode, however, is not seriously limited by these factors.

A complication of the Boeing-ERL meteor-burst time synchronization system is the requirement for a transmitter-receiver pair at each terminal of the link. The slave station, however, must transmit a pulse train only upon interrogation, and then requires modest power and a rather simple VHF antenna. The operational range is such that six master stations could synchronize the entire United States, while the use of moderately directional antennas reduces the probability of interchannel interference.

Conclusions

In summary, the results presented here indicate that VHF signals reflected from meteor trails exhibit extremely stable phase characteristics. For average trail durations, changes in propagation path delays are less than twenty nanoseconds for individual trails, and, for the 550-mile link described, variations from trail to trail could be placed in a 200 microsecond time block.

The experiments indicate that the medium itself would not be the limiting factor in time synchronization systems capable of accuracies on the order of a few hundred nanoseconds. In addition, the feasibility of a meteor-burst instantaneous time synchronization system has been established by the first manual system which, even though rather crude, still was capable of synchronization accuracies on the order of 10–20 microseconds. The automatic system, currently under construction, should greatly improve upon this figure.

Rainfall Attenuation of Centimeter Waves: Comparison of Theory and Measurement

RICHARD G. MEDHURST

Abstract—**Numerical results for attenuation of centimeter waves by rainfall have been computed from J. W. Ryde's formula. These correct, and considerably extend, the previously published Ryde results. Comparison with available measurements suggests that the agreement is not entirely satisfactory; there is a tendency for measured attenuations to exceed the maximum possible levels predicted by the theory.**

I. Introduction

AT PRESENT, UHF/SHF line-of-sight radio relay systems operate in frequency bands in the neighborhood of 2 Gc/s, 4 Gc/s, 6 Gc/s, and, most recently, 11 Gc/s. Also available, and under consideration, is a band at 18 Gc/s. Attenuation by rainfall is of no importance in the 2-Gc/s band, but can become of increasing concern as the frequency increases. At 11 Gc/s rainfall attenuation may represent a severe limitation on system performance. Prediction of the effects of rainfall in a location in which it is proposed to install a radio link thus becomes important; this may be the deciding factor in the choice of operating frequency.

A theoretical approach to this problem was developed by J. W. Ryde [1]–[3] during World War II, and has formed the basis of much subsequent work. However, attempts to deduce attenuation levels from Ryde's results, for the frequencies previously mentioned, showed that the parameter values chosen by Ryde were too widely spaced to permit reliable interpolation. Consequently, it was decided to carry through the Ryde computation for a much more comprehensive series of parameter values. Differences appeared between the newly computed results and those of Ryde, et al. [3]; the discrepancy being traced to the necessity in the early work (which was done under pressing war-time conditions and without modern aids of computation)

Manuscript received November 16, 1964; revised March 5, 1965.
The author is with the Telecommunications Research Labs., Hirst Research Centre, General Electric Co., Ltd., Wembley, England.

of basing certain intermediate curves on an inadequate number of points.

The present computed values cover the wavelength range from 0.3 to 15 cm, and precipitation intensities from 0.25 to 150 mm/hour, and are at intervals sufficiently close to allow accurate interpolation.

The theoretical figures are for uniform rainfall along the path between transmitting and receiving antennas. Prediction of the performance of actual links depends on knowledge of the way in which rainfall intensity tends to vary along the path (which may be of the order of 30 miles in length). A working basis for this is suggested by Bussey [4], but it appears that meteorological information is quite inadequate, and there is a need for a great deal of systematic measurement of instantaneous rainfall intensity distributions over large areas, under various climatic conditions. The results of measurements of this kind would provide a firmer basis for predicting attenuations under operational conditions in climatic regions similar to those in which the rainfall intensity distributions were determined, though the picture in other regions (e.g., tropical) may well be substantially different.

No systematic comparison seems to have been made between the theoretically predicted rainfall attenuation levels and those found by experiment. This has been done here for all sets of measurements (made under sufficiently well-defined meteorological conditions) which could be located in the literature. It appears that the agreement is not completely satisfactory. Almost always a wide scatter of points is reported. In many cases, a substantial proportion of the points lies within the extreme possible limits of theoretically predicted attenuation, but there is a marked tendency for observed attenuations to fall *well above* levels which, according to the theory, cannot be exceeded.

II. Theoretical Evaluation of Attenuation by Rainfall

The analysis in [1]–[3] is based on the following:

$$\text{Attenuation} = 4.343 \frac{N\lambda^2}{2\pi} A_i 10^5 \text{ dB/km}, \qquad (1)$$

for a hypothetical rain consisting of drops of equal diameter; the drop concentration supposedly uniform. In this expression,

N = number of drops per cubic centimeter

λ = wavelength (cm)

$$A_i = \text{real part of } \sum_{n=1}^{\infty} (a_n + p_n)$$

where

$$a_n = (2n+1)\left[\frac{S_n(\alpha)S_n'(m\alpha) - mS_n'(\alpha)S_n(m\alpha)}{\phi_n(\alpha)S_n'(m\alpha) - m\phi_n'(\alpha)S_n(m\alpha)}\right]$$

$$p_n = (2n+1)\left[\frac{mS_n(\alpha)S_n'(m\alpha) - S_n'(\alpha)S_n(m\alpha)}{m\phi_n(\alpha)S_n'(m\alpha) - \phi_n'(\alpha)S_n(m\alpha)}\right]$$

$$S_n(x) = \sqrt{\frac{\pi}{2}\, x J_{n+1/2}(x)}$$

$$C_n(x) = (-1)^n \sqrt{\frac{\pi}{2}\, x J_{-(n+1/2)}(x)}$$

$J_\nu(x)$ = the Bessel function of the first kind of order ν

$\phi_n(x) = S_n(x) + jC_n(x)$

$\alpha = \pi D/\lambda$

D = drop diameter (cm)

$m = \eta - j\eta\chi$ = square root of the complex dielectric constant of water.

Expression (1) (first given by G. Mie in 1908 [26]), is derived [28] by considering the interaction of a plane wavefront with a single spherical drop. It is assumed that the total attenuation is proportional to N. Necessary conditions for this to hold appear to be 1) that the drops are randomly scattered, with uniform average density, throughout the space between transmitting and receiving antennas, 2) that the assumption of a plane wavefront at each drop position is adequate (this is clearly not so in the near-field region of each antenna), and 3) that interaction between drops is negligible.[1]

The fundamental physical quantity in (1) is m. Saxton [5] gives the following semi-empirical expressions for the real and imaginary parts of m:

$$\eta = \frac{1}{\sqrt{2}}\left\{\sqrt{\frac{\epsilon_s^2 + \epsilon_0^2 x^2}{1+x^2}} + \frac{\epsilon_s + \epsilon_0 x^2}{1+x^2}\right\}^{1/2}$$

$$\eta\chi = \frac{1}{\sqrt{2}}\left\{\sqrt{\frac{\epsilon_s^2 + \epsilon_0^2 x^2}{1+x^2}} - \frac{\epsilon_s + \epsilon_0 x^2}{1+x^2}\right\}^{1/2} \qquad (2)$$

where

$$x = \omega\tau_0 = \frac{2\pi \times 3 \times 10^{10}}{\lambda}\tau_0.$$

Saxton recommends that ϵ_0 be taken as 5.5. τ_0, which is temperature dependent, is to be read from Fig. 4 of Saxton [5], and ϵ_s, also temperature dependent, from Table 3 of Saxton [5], or Table 4 of Lattey et al., [6]. At 20°C, $\tau_0 = 8.1 \times 10^{-12}$, $\epsilon_s = 80.08$. Table I gives some computed values of m for this temperature.

In order to relate the attenuation to the precipitation rate p mm/hour, rather than to N (the average number of drops per cm^3), it is necessary to have a relationship between N and p. This involves the terminal velocity of the drops (which is dependent on the drop diameter). It is readily shown that

$$p = 6\pi \times 10^5 v N D^3$$

$$= 1.885 \times 10^6 v N D^3 \text{ mm/hour} \qquad (3)$$

where v is the terminal velocity in meters per second.

[1] This is stated by Ryde [2], p 3, to be an allowable assumption when the distance between drops is greater than five times their diameter, as normally will be the case.

TABLE I

REFRACTIVE AND ABSORPTION INDEXES FOR WATER AT 20°C

λ (cm)	$m=\eta-j\eta\chi$	
	η	$\eta\chi$
0.3	3.509	2.010
0.5	4.370	2.524
1.0	6.000	2.849
3.0	8.251	1.827
5.0	8.670	1.202
10.0	8.875	0.627
15.0	8.916	0.422

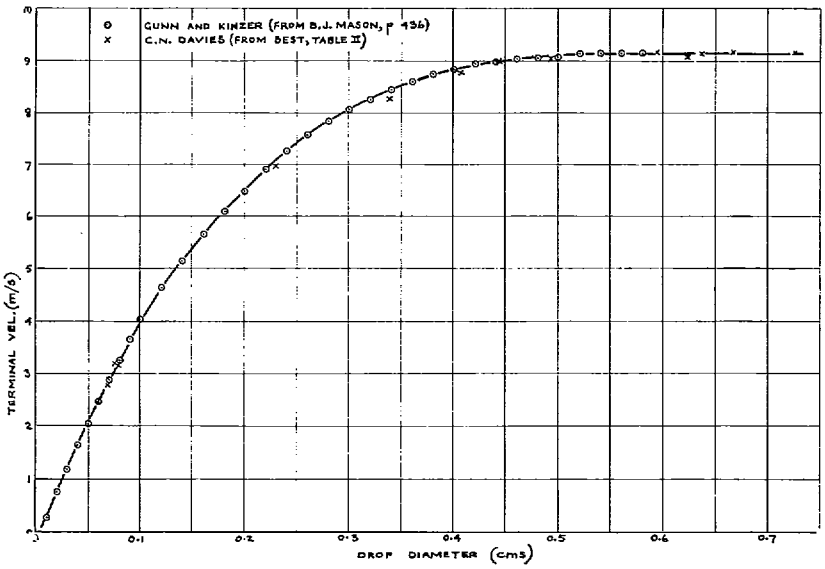

Fig. 1. Terminal velocity of raindrops as a function of drop diameter.

TABLE II

TERMINAL VELOCITIES OF DROPS OF VARIOUS SIZES

D (cm)	v (m/s)	$p=1.885vD^3 10^6$ (mm/hour for $N=1$)
0.05	2.06	4.854×10^2
0.10	4.03	7.597×10^3
0.15	5.40	3.435×10^4
0.20	6.49	9.787×10^4
0.25	7.41	2.182×10^5
0.30	8.06	4.102×10^5
0.35	8.53	6.894×10^5
0.40	8.83	1.065×10^6
0.45	9.00	1.546×10^6
0.50	9.09	2.142×10^6
0.55	9.13	2.863×10^6
0.60	9.14	3.721×10^6
0.65	9.14	4.731×10^6
0.70	9.14	5.910×10^6

TABLE III

DROP-SIZE DISTRIBUTIONS FOR VARIOUS PRECIPITATION RATES

Drop size (cm) (mean in interval) \ Precipitation rate (mm/hour)	Percent of total volume								
	0.25	1.25	2.5	5	12.5	25	50	100	150
0.05	28.0	10.9	7.3	4.7	2.6	1.7	1.2	1.0	1.0
0.1	50.1	37.1	27.8	20.3	11.5	7.6	5.4	4.6	4.1
0.15	18.2	31.3	32.8	31.0	24.5	18.4	12.5	8.8	7.6
0.2	3.0	13.5	19.0	22.2	25.4	23.9	19.9	13.9	11.7
0.25	0.7	4.9	7.9	11.8	17.3	19.9	20.9	17.1	13.9
0.3		1.5	3.3	5.7	10.1	12.8	15.6	18.4	17.7
0.35		0.6	1.1	2.5	4.3	8.2	10.9	15.0	16.1
0.4		0.2	0.6	1.0	2.3	3.5	6.7	9.0	11.9
0.45			0.2	0.5	1.2	2.1	3.3	5.8	7.7
0.5				0.3	0.6	1.1	1.8	3.0	3.6
0.55					0.2	0.5	1.1	1.7	2.2
0.6						0.3	0.5	1.0	1.2
0.65							0.2	0.7	1.0
0.7									0.3

Values of v are shown plotted in Fig. 1.[2] Terminal velocities read from the curve of Fig. 1 are given in Table II.

Finally, to relate attenuation to an actual rainstorm (rather than to a fictitious one consisting of equal-size drops), it is necessary to know the drop-size distribution in rain of given intensity. This will vary according to wind, temperature, and other conditions (e.g., see Grunow [9]). Representative distributions were obtained by Laws and Parsons [10], during 1938 and 1939, in Washington D. C. Table III is abridged from their Table 3, with the addition of a distribution for a precipitation rate of 5 mm/hour, which has been derived from their Fig. 1.

To evaluate the effect of the drop-size distribution, suppose that for a particular precipitation rate, say p mm/hour, p_D is the proportion of the total volume of water reaching the ground which consists of drops whose diameters fall in the interval centered on D cm. Then, from (3),

$$N_D = \frac{p \cdot p_D}{1.885 \times 10^6 v D^3}.$$

If the decibel loss/kilometer for a rain concentration of one drop per cubic centimeter, with a uniform drop diameter of D cm, is d_D [given by (1) with the omission of the term N], the total attenuation is

$$\sum_D \frac{d_D p_D p}{1.885 \times 10^6 v D^3},$$

i.e.,

$$p \sum_D \left(\frac{d_D}{1.885 \times 10^6 v D^3} \right) p_D \text{ dB/km.} \qquad (4)$$

[2] Values of v are taken from Mason [7], p 436, and from Best [8].

Relations (1) and (4) are essentially those developed by Mssrs. Ryde [3], and they form the basis of the numerical work reported in that reference. Both these formulas and the numerical results of Ryde, et al. [3] have been extensively quoted. In Al'pert [11], for example, Ryde's tables are copied exactly, though without acknowledgment (Ryde's name is not mentioned, even in the extensive bibliography appended to Al'pert [11]).

Since the attenuation values tabulated in Ryde, et al. [3] were not computed at sufficiently close intervals to permit interpolation with acceptable accuracy (especially in the 5-cm wavelength region), it was decided to repeat the computation on a more extensive scale. Due to the current availability of electronic computers, this was a much easier task than that confronting the authors of [3]. It appears that during most of the period when the original work was undertaken, there were not even available tables of Bessel functions of real argument of order $n+\frac{1}{2}$. These functions had all to be computed from the complicated trigonometrical/algebraic expressions that represented them.

A_i in (1) was evaluated for a wide range of conditions with the help of a Hollerith Hec. 2M computer. Chosen values of λ were 0.3, 0.5, 1, 2, 3, 5, 10, and 15 cm. At each λ, A_i was evaluated for α, taken in steps of 0.05, over a range sufficient to cover D values in the interval 0.05 (0.05) 0.70 cm. To interpolate for intermediate values of λ, it was found convenient to plot d_D [as in (4)] against λ, on a log per log scale, for the various values of α. A smooth curve, approaching a straight line, is obtained in each case, and for particular λ's, these curves yield d_D values at fairly closely spaced values of D. These are then plotted against D, and d_D is read for the D values required.

The Bessel functions of order $n+\frac{1}{2}$ and complex argument, required for evaluation of A_i, were obtained in two ways. For the smaller α values, use was made of a Taylor series expansion of the function in powers of the

imaginary part of the argument. By this device, the function is represented by a fairly rapidly converging series involving Bessel functions of real argument only. For the larger α's, recourse was had to a recurrence formula previously used by Aden [12]. Writing F_n for $S_n'(x)/S_n(x)$, it may readily be shown that

$$F_n = \frac{1 - \frac{n}{x}\left(\frac{n}{x} - F_{n-1}\right)}{\frac{n}{x} - F_{n-1}}.$$

This is a somewhat surprising relation since it connects only two F's of consecutive order, whereas recurrence formulas for Bessel functions generally involve three such functions.

Considering a hypothetical rain of uniform drop size, the most physically meaningful quantity to tabulate will be the bracketed quantity in (4). This may be interpreted as the attenuation due to precipitation at the rate of one mm/hour, when the drop sizes are equal and of the diameter specified. Numerical values are given in Table IV, which replaces Table 7 of Ryde, et al. [3].

It is evident from the form of (4) that the maximum and minimum possible attenuations predicted by the present theory will result when the precipitation is composed of drops all of the same size, D being such that for the particular λ the entry in Table IV has, respectively, its largest and smallest value.

These maxima and minima are given in the bottom two rows of Table IV. They sometimes fall outside the range of the entries in the upper rows; this is because they were read from curves plotted for each λ, and these curves in some cases show sharp peaking, the peaks lying between the D values tabulated. It will be appreciated that precipitations in which the drop sizes are substantially equal are most unlikely to be encountered, so that these theoretical maxima and minima represent extreme outside limits.

Figure 2 shows curves of theoretical maximum and minimum attenuations. The attenuation, in these cases, is proportional to the precipitation rate. The discontinuities of slope in the lower curve at $\lambda = 1$ cm and the upper curve at $\lambda = 6$ cm occur because in these regions the drop size for minimum or maximum attenuation jumps from one end of the range of D to the other (measurements of drop sizes in precipitations show that D never exceeds 0.7 cm).

The data in Table III and Table IV can now be combined according to (4) to give the attenuation as a function of precipitation rate and wavelength, when the Laws and Parsons drop-size distribution is assumed. The results are shown in Table V. Interpolated values, from this table, for the frequencies used in trunk radio systems, are shown plotted in Fig. 3.

III. Effect of Departure of the Raindrop Shape from Spherical

It has been observed by photographic methods that raindrops are not truly spherical (as assumed in Ryde's theory) but tend to be flattened, or even to become concave, at the base, the amount of flattening increasing with the size of the drop. For this reason, it would be expected that the attenuation would be sensitive to the polarization of the radio wave.

Oguchi [13] has computed the theoretically expected change in the attenuation of 8.6 mm waves from that due to spherical drops when the drops are actually spheroidal, with a theoretically predicted eccentricity, at terminal velocity. Table VI is a modification of his Table 4, and shows the percentage change from the Ryde values (based on the Laws and Parsons drop-size distribution).

It is seen that at this wavelength the error due to deformation of the raindrops is not expected to exceed 16 per cent. This, as will appear in Section V, is considerably less than some of the discrepancies between the theoretical and measured values.

IV. Effect of Temperature

Two of the quantities appearing in (2), for the complex dielectric constant of water, are temperature dependent. Consequently, the theoretical attenuation levels will also depend on temperature. Ryde has computed correction factors (Table XVI of Ryde et al. [3]) to allow for this temperature effect. His table, with a slight modification, is reproduced here as Table VII.

The correction factors in Table VII seem not to show any very clear trend. In the temperature range 10 to 30°C, and for wavelengths of three cm or less, they do not exceed ± 20 percent, and are generally much less.

V. Measured Rainfall Attenuations

The usual procedure for measurement of rainfall attenuation has been the straightforward one of setting up transmitting and receiving antennas at the ends of a line-of-sight path, and locating along the path what is hoped to be an adequate number of rain gauges. All but one of the sets of measurements discussed here were carried out in this way. An immediate difficulty that presents itself consists of a conflicting requirement on the antenna spacing: unless the antennas are spaced apart by a substantial distance, the rainfall attenuation will be too small to be measurable, particularly at the lower frequencies, but as the spacing is incremented, it becomes increasingly less likely that at any instant the precipitation will be uniform along the path.

Another difficulty involves the response time of the rain gauges, and the coordination in time of the instantaneous rain gauge readings with the measurement of the radio wave attenuation. Whereas the measured attenuation changes virtually instantaneously as the precipitation rate fluctuates, the rain gauge, which is normally a device for collecting a sample of the precipitation and delivering it to a graduated measure, will show considerable lag when precipitation fluctuations are rapid.

Yet another source of error is the effect of wind. The rain gauges normally present a horizontal collecting area; under conditions of wind, and especially gusty

TABLE IV

ATTENUATION IN dB/KM DUE TO PRECIPITATION AT THE RATE OF 1 MM/HOUR, COMPOSED OF DROPS OF EQUAL DIAMETER D (TEMPERATURE 20°C)

Drop diameter (cm)	Wavelength (cm)															
	0.3	0.5	1	1.5	2	3	4	5	5.5	6	6.5	7	8	9	10	15
0.05	1.85	0.46	0.97 $\times 10^{-1}$	0.43 $\times 10^{-1}$	0.19 $\times 10^{-1}$	0.75 $\times 10^{-2}$	0.34 $\times 10^{-2}$	0.24 $\times 10^{-2}$	0.13 $\times 10^{-2}$	0.10 $\times 10^{-2}$	0.85 $\times 10^{-3}$	0.71 $\times 10^{-3}$	0.54 $\times 10^{-3}$	0.45 $\times 10^{-3}$	0.40 $\times 10^{-3}$	0.25 $\times 10^{-3}$
0.10	1.49	0.74	0.14	0.48 $\times 10^{-1}$	0.18 $\times 10^{-1}$	0.59 $\times 10^{-2}$	0.28 $\times 10^{-2}$	0.15 $\times 10^{-2}$	0.12 $\times 10^{-2}$	0.94 $\times 10^{-3}$	0.76 $\times 10^{-3}$	0.63 $\times 10^{-3}$	0.46 $\times 10^{-3}$	0.36 $\times 10^{-3}$	0.29 $\times 10^{-3}$	0.13 $\times 10^{-3}$
0.15	0.66	0.68	0.20	0.77 $\times 10^{-1}$	0.34 $\times 10^{-1}$	0.72 $\times 10^{-2}$	0.28 $\times 10^{-2}$	0.15 $\times 10^{-2}$	0.12 $\times 10^{-2}$	0.93 $\times 10^{-3}$	0.74 $\times 10^{-3}$	0.61 $\times 10^{-3}$	0.43 $\times 10^{-3}$	0.32 $\times 10^{-3}$	0.25 $\times 10^{-3}$	0.10 $\times 10^{-3}$
0.20	0.41	0.42	0.22	0.12	0.63 $\times 10^{-1}$	0.13 $\times 10^{-1}$	0.40 $\times 10^{-2}$	0.18 $\times 10^{-2}$	0.13 $\times 10^{-2}$	0.10 $\times 10^{-2}$	0.80 $\times 10^{-3}$	0.64 $\times 10^{-3}$	0.42 $\times 10^{-3}$	0.30 $\times 10^{-3}$	0.23 $\times 10^{-3}$	0.91 $\times 10^{-4}$
0.25	0.28	0.28	0.22	0.11	0.88 $\times 10^{-1}$	0.24 $\times 10^{-1}$	0.60 $\times 10^{-2}$	0.23 $\times 10^{-2}$	0.16 $\times 10^{-2}$	0.12 $\times 10^{-2}$	0.91 $\times 10^{-3}$	0.73 $\times 10^{-3}$	0.47 $\times 10^{-3}$	0.31 $\times 10^{-3}$	0.24 $\times 10^{-3}$	0.86 $\times 10^{-4}$
0.30	0.21	0.21	0.21	0.11	0.74 $\times 10^{-1}$	0.44 $\times 10^{-1}$	0.98 $\times 10^{-2}$	0.34 $\times 10^{-2}$	0.23 $\times 10^{-2}$	0.15 $\times 10^{-2}$	0.11 $\times 10^{-2}$	0.89 $\times 10^{-3}$	0.55 $\times 10^{-3}$	0.36 $\times 10^{-3}$	0.27 $\times 10^{-3}$	0.87 $\times 10^{-4}$
0.35	0.17	0.17	0.18	0.11	0.71 $\times 10^{-1}$	0.67 $\times 10^{-1}$	0.19 $\times 10^{-1}$	0.51 $\times 10^{-2}$	0.32 $\times 10^{-2}$	0.21 $\times 10^{-2}$	0.15 $\times 10^{-2}$	0.11 $\times 10^{-2}$	0.67 $\times 10^{-3}$	0.43 $\times 10^{-3}$	0.31 $\times 10^{-3}$	0.91 $\times 10^{-4}$
0.40	0.14	0.14	0.15	0.11	0.71 $\times 10^{-1}$	0.49 $\times 10^{-1}$	0.35 $\times 10^{-1}$	0.83 $\times 10^{-2}$	0.47 $\times 10^{-2}$	0.30 $\times 10^{-2}$	0.21 $\times 10^{-2}$	0.15 $\times 10^{-2}$	0.84 $\times 10^{-3}$	0.53 $\times 10^{-3}$	0.36 $\times 10^{-3}$	0.99 $\times 10^{-4}$
0.45	0.12	0.12	0.12	0.12	0.72 $\times 10^{-1}$	0.41 $\times 10^{-1}$	0.57 $\times 10^{-1}$	0.16 $\times 10^{-1}$	0.87 $\times 10^{-2}$	0.47 $\times 10^{-2}$	0.30 $\times 10^{-2}$	0.20 $\times 10^{-2}$	0.11 $\times 10^{-2}$	0.66 $\times 10^{-3}$	0.43 $\times 10^{-3}$	0.11 $\times 10^{-3}$
0.50	0.10	0.11	0.11	0.11	0.75 $\times 10^{-1}$	0.40 $\times 10^{-1}$	0.44 $\times 10^{-1}$	0.32 $\times 10^{-1}$	0.16 $\times 10^{-1}$	0.78 $\times 10^{-2}$	0.46 $\times 10^{-2}$	0.29 $\times 10^{-2}$	0.15 $\times 10^{-2}$	0.83 $\times 10^{-3}$	0.53 $\times 10^{-3}$	0.12 $\times 10^{-3}$
0.55	0.92 $\times 10^{-1}$	0.96 $\times 10^{-1}$	0.99 $\times 10^{-1}$	0.97 $\times 10^{-1}$	0.78 $\times 10^{-1}$	0.41 $\times 10^{-1}$	0.34 $\times 10^{-1}$	0.51 $\times 10^{-1}$	0.26 $\times 10^{-1}$	0.14 $\times 10^{-1}$	0.81 $\times 10^{-2}$	0.44 $\times 10^{-2}$	0.20 $\times 10^{-2}$	0.11 $\times 10^{-2}$	0.67 $\times 10^{-3}$	0.14 $\times 10^{-3}$
0.60	0.83 $\times 10^{-1}$	0.87 $\times 10^{-1}$	0.91 $\times 10^{-1}$	0.88 $\times 10^{-1}$	0.83 $\times 10^{-1}$	0.42 $\times 10^{-1}$	0.29 $\times 10^{-1}$	0.48 $\times 10^{-1}$	0.47 $\times 10^{-1}$	0.23 $\times 10^{-1}$	0.14 $\times 10^{-1}$	0.84 $\times 10^{-2}$	0.28 $\times 10^{-2}$	0.14 $\times 10^{-2}$	0.87 $\times 10^{-3}$	0.16 $\times 10^{-3}$
0.65	0.76 $\times 10^{-1}$	0.79 $\times 10^{-1}$	0.83 $\times 10^{-1}$	0.82 $\times 10^{-1}$	0.95 $\times 10^{-1}$	0.46 $\times 10^{-1}$	0.28 $\times 10^{-1}$	0.30 $\times 10^{-1}$	0.45 $\times 10^{-1}$	0.41 $\times 10^{-1}$	0.22 $\times 10^{-1}$	0.14 $\times 10^{-1}$	0.42 $\times 10^{-2}$	0.19 $\times 10^{-2}$	0.11 $\times 10^{-2}$	0.19 $\times 10^{-3}$
0.70	0.70 $\times 10^{-1}$	0.73 $\times 10^{-1}$	0.77 $\times 10^{-1}$	0.77 $\times 10^{-1}$	0.77 $\times 10^{-1}$	0.51 $\times 10^{-1}$	0.27 $\times 10^{-1}$	0.23 $\times 10^{-1}$	0.30 $\times 10^{-1}$	0.48 $\times 10^{-1}$	0.41 $\times 10^{-1}$	0.21 $\times 10^{-1}$	0.68 $\times 10^{-2}$	0.26 $\times 10^{-2}$	0.14 $\times 10^{-2}$	0.22 $\times 10^{-3}$
Maximum attenuation	2.37	0.76	0.22	0.12	0.95 $\times 10^{-1}$	0.68 $\times 10^{-1}$	0.58 $\times 10^{-1}$	0.53 $\times 10^{-1}$	0.54 $\times 10^{-1}$	0.53 $\times 10^{-1}$	0.22 $\times 10^{-1}$	0.14 $\times 10^{-1}$	0.42 $\times 10^{-2}$	0.19 $\times 10^{-2}$	0.11 $\times 10^{-2}$	0.25 $\times 10^{-3}$
Minimum attenuation	0.76 $\times 10^{-1}$	0.79 $\times 10^{-1}$	0.83 $\times 10^{-1}$	0.40 $\times 10^{-1}$	0.17 $\times 10^{-1}$	0.59 $\times 10^{-2}$	0.27 $\times 10^{-2}$	0.15 $\times 10^{-2}$	0.12 $\times 10^{-2}$	0.93 $\times 10^{-3}$	0.74 $\times 10^{-3}$	0.61 $\times 10^{-3}$	0.40 $\times 10^{-3}$	0.30 $\times 10^{-3}$	0.23 $\times 10^{-3}$	0.86 $\times 10^{-4}$

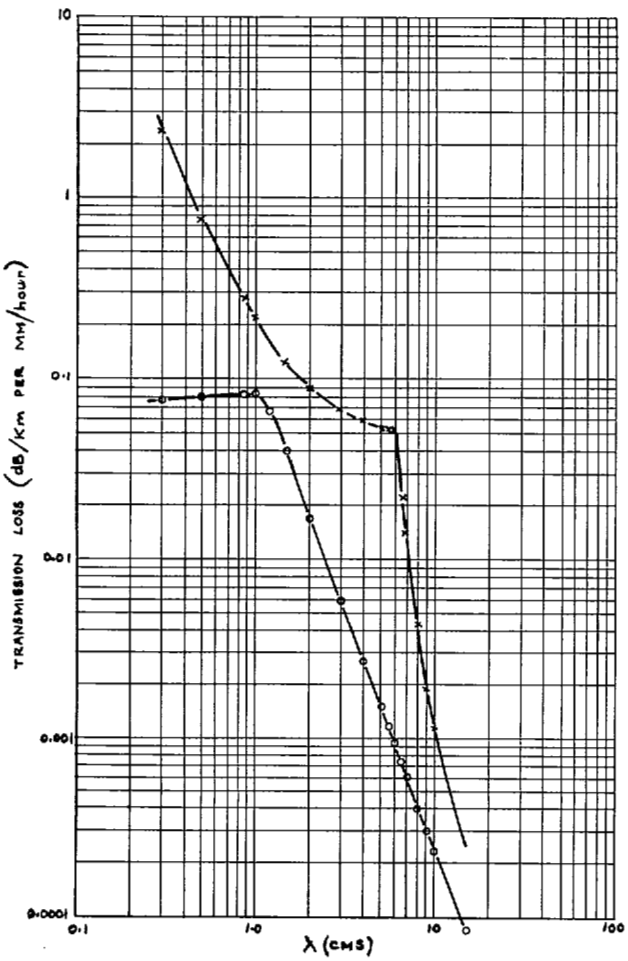

Fig. 2. Theoretical maximum and minimum attenuations due to rainfall.

TABLE V

ATTENUATION IN DB/KM FOR VARIOUS RATES OF PRECIPITATION ASSUMING THE LAWS AND PARSONS' DROP-SIZE DISTRIBUTION (TEMPERATURE 20°C)

Precipitation rate (mm/hour)	Wavelength (cm)															
	0.3	0.5	1	1.5	2	3	4	5	5.5	6	6.5	7	8	9	10	15
0.25	0.250	0.159	0.349 $\times 10^{-1}$	0.136 $\times 10^{-1}$	0.572 $\times 10^{-2}$	0.172 $\times 10^{-2}$	0.757 $\times 10^{-3}$	0.442 $\times 10^{-3}$	0.309 $\times 10^{-3}$	0.242 $\times 10^{-3}$	0.196 $\times 10^{-3}$	0.162 $\times 10^{-3}$	0.119 $\times 10^{-3}$	0.939 $\times 10^{-4}$	0.780 $\times 10^{-4}$	0.396 $\times 10^{-4}$
1.25	1.29	0.764	0.210	0.878 $\times 10^{-1}$	0.423 $\times 10^{-1}$	0.116 $\times 10^{-1}$	0.431 $\times 10^{-2}$	0.218 $\times 10^{-2}$	0.160 $\times 10^{-2}$	0.123 $\times 10^{-2}$	0.986 $\times 10^{-3}$	0.809 $\times 10^{-3}$	0.572 $\times 10^{-3}$	0.434 $\times 10^{-3}$	0.350 $\times 10^{-3}$	0.159 $\times 10^{-3}$
2.5	2.19	1.43	0.447	0.196	0.100	0.284 $\times 10^{-1}$	0.101 $\times 10^{-1}$	0.465 $\times 10^{-2}$	0.339 $\times 10^{-2}$	0.257 $\times 10^{-2}$	0.203 $\times 10^{-2}$	0.165 $\times 10^{-2}$	0.112 $\times 10^{-2}$	0.851 $\times 10^{-3}$	0.678 $\times 10^{-3}$	0.294 $\times 10^{-3}$
5	3.68	2.63	0.933	0.427	0.233	0.718 $\times 10^{-1}$	0.252 $\times 10^{-1}$	0.107 $\times 10^{-1}$	0.749 $\times 10^{-2}$	0.554 $\times 10^{-2}$	0.430 $\times 10^{-2}$	0.346 $\times 10^{-2}$	0.234 $\times 10^{-2}$	0.170 $\times 10^{-2}$	0.133 $\times 10^{-2}$	0.550 $\times 10^{-3}$
12.5	7.08	5.46	2.43	1.18	0.709	0.240	0.848 $\times 10^{-1}$	0.336 $\times 10^{-1}$	0.226 $\times 10^{-1}$	0.159 $\times 10^{-1}$	0.120 $\times 10^{-1}$	0.941 $\times 10^{-2}$	0.586 $\times 10^{-2}$	0.429 $\times 10^{-2}$	0.330 $\times 10^{-2}$	0.128 $\times 10^{-2}$
25	11.7	9.86	4.87	2.49	1.53	0.602	0.223	0.882 $\times 10^{-1}$	0.580 $\times 10^{-1}$	0.383 $\times 10^{-1}$	0.279 $\times 10^{-1}$	0.213 $\times 10^{-1}$	0.127 $\times 10^{-1}$	0.900 $\times 10^{-2}$	0.678 $\times 10^{-2}$	0.247 $\times 10^{-2}$
50	19.6	17.0	9.59	5.15	3.28	1.45	0.590	0.235	0.152	0.971 $\times 10^{-1}$	0.678 $\times 10^{-1}$	0.499 $\times 10^{-1}$	0.283 $\times 10^{-1}$	0.194 $\times 10^{-1}$	0.142 $\times 10^{-1}$	0.489 $\times 10^{-2}$
100	33.7	29.4	18.4	10.4	6.77	3.43	1.55	0.639	0.416	0.260	0.174	0.123	0.659 $\times 10^{-1}$	0.432 $\times 10^{-1}$	0.309 $\times 10^{-1}$	0.989 $\times 10^{-2}$
150	46.8	40.9	26.8	15.7	10.2	5.49	2.71	1.13	0.739	0.472	0.313	0.214	0.110	0.700 $\times 10^{-1}$	0.492 $\times 10^{-1}$	0.151 $\times 10^{-1}$

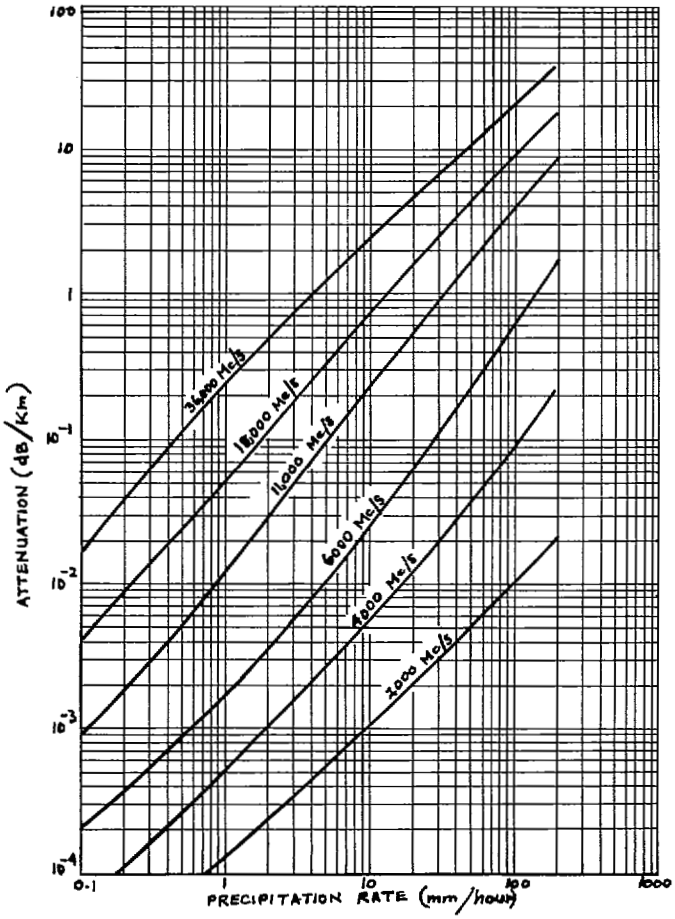

Fig. 3. Theoretical rainfall attenuation (various frequencies).

TABLE VI

EXPECTED PERCENTAGE CHANGE IN THE RYDE THEORETICAL ATTENUATIONS AT 8.6 MM DUE TO DEPARTURE OF THE DROP SHAPE FROM SPHERICAL (AFTER OGUCHI [13])

Precipitation rate (mm/hour)	Percentage change in attenuation (measured in dB/km)	
	Vertical polarization	Horizontal polarization
0.25	−4.9	+2.5
1.25	−7.8	+2.4
2.5	−8.9	+2.5
12.5	−11.7	+2.2
25	−13.2	+0.3
50	−14.6	+1.7
100	−15.9	+0.9
150	−15.9	+1.0

TABLE VII

EXPECTED PERCENTAGE CHANGE IN THE RYDE THEORETICAL ATTENUATIONS DUE TO TEMPERATURE CHANGES (REFERRED TO THE ATTENUATION AT 18°C) (AFTER RYDE [3])

Precipitation rate (mm/hour)	λ (cm)	Percentage change in attenuation (measured in dB/km)				
		$T=0°C$	$T=10°C$	$T=18°C$	$T=30°C$	$T=40°C$
0.25	0.5	−15	−5	0	+2	−1
	1.25	−5	0	0	−10	−19
	3.2	+21	+10	0	−21	−45
	10	+101	+40	0	−30	−41
2.5	0.5	−13	−5	0	+3	+1
	1.25	−15	−1	0	−8	−20
	3.2	−18	+1	0	−18	−36
	10	+102	+40	0	−30	−41
12.5	0.5	−10	−4	0	+2	0
	1.25	−17	−4	0	−7	−19
	3.2	−36	−12	0	−10	−30
	10	+103	+40	0	−30	−41
50	0.5	−6	−2	0	+1	0
	1.25	−16	−5	0	−5	−17
	3.2	−38	−13	0	−1	−19
	10	+101	+40	0	−30	−42
150	0.5	−4	−2	0	+1	0
	1.25	−14	−4	0	−3	−13
	3.2	−34	−12	0	+3	−11
	10	+100	+40	0	−30	−42

wind, it would seem likely that the water density in the air, for a given precipitation rate on the ground, will be different from what it would be during calm periods.

No rainfall attenuation measurements have been recorded for wavelengths greater than 3.2 cm. An attempt was made by Wolff and Linder [14] to measure rainfall attenuation of 9-cm waves over a two-mile path, but they found no detectable effect, and concluded that the attenuation was less than 0.1 dB per mile.

Table VIII summarizes the available published information on rainfall attenuation measurements. It will be apparent from the final column that these measurements are of varying degrees of reliability. In no case is the ambient temperature recorded. However, Table VII shows that for these short wavelengths temperature effects would not be expected to be large.

All the measured points given in [15]–[25] are displayed in Figs. 4–18. In each figure is shown the maximum and minimum theoretical attenuations (full lines), taken from Fig. 2, as well as the theoretical curve (broken line), based on the Laws and Parsons drop-size distribution, taken from Table V. It will be seen that in the majority of cases there is a marked tendency for measured attenuation values to fall *above* the maximum possible predicted by the theory, often by a considerable margin. Attention is called particularly to the measurements of Anderson, et al. (Fig. 6), which seem to have been conducted with unusual care.

Thus, the applicability of the Mie theory to the practical rainfall situation cannot be said to be demonstrated. In view of this, and also of the very large scatter in the measured points that is often observed, the attenuation curves obtained by applying the Mie theory to the Laws and Parsons drop-size distribution can only be taken as giving a rather crude order of magnitude.

An attempt was made to derive empirical bounds and means for rainfall attenuation. The Ryde theory predicts that at a particular wavelength the attenuation will not be strictly proportional to the precipitation rate, the reason for this being the variation in drop-size distribution with precipitation rate. However, in most of the sets of measurements, the scatter of points is such that any more refined assumption than a linear dependence of attenuation on precipitation rate is not justified. Assuming a linear dependence, two lines of appropriate slope were drawn on each figure enclosing approximately 90 percent of the measured points. Proportionality constants relating attenuation to precipitation rate were obtained from these, and are shown plotted in Figs. 19 and 20. Curves based on Mie's formula, as used in Ryde's theory, are also shown. Even allowing for the very considerable scatter of points, it is clear that the Ryde limiting curves tend very much to underestimate both the upper and lower limits of attenuation.

Figure 21 shows mean attenuations for each set of measurements obtained by averaging the upper and lower limits displayed in Figs. 19 and 20. Also included is a point based on the measurements reported in Anderson, et al. [17] and reproduced in Fig. 6. These latter measurements give points lying so closely on a straight line that there would have been no point in plotting upper and lower limits.

Lines drawn to lie evenly among the points of Figs. 19, 20, and 21 are shown in Fig. 22. It will be noticed that the "mean" line does not lie everywhere halfway (linearly) between the two extreme lines. This is largely due to the considerable weight that has been given to the results from Anderson, et al. [17]. In the present state of knowledge, it would appear that these curves form the best available basis for system design.

TABLE VIII

PUBLISHED MEASUREMENTS OF RAINFALL ATTENUATION OF MICROWAVE RADIATION

Reference number	Figure number	Authors	Wavelength (cm)	Polarization	Path length	Number of rain gauges	Remarks
[15]	12	Robertson and King	3.2	Horizontal	900 feet	1	These measurements were made during two storms only. In one, the rain gauge was about 1000 feet from the transmitter, and, in the other, about 500 feet from the receiver, in each case on a line perpendicular to the transmission path. The rain gauge gave average intensity over about one minute.
[16]	13	Hathaway and Evans	2.63	Not stated	27.7 miles	13	The rain gauges were spaced at approximately two-mile intervals. It was assumed that the rainfall was uniform for one mile each side of a rain gauge, and the measurements were reduced to give the attenuation for rain of uniform intensity by a semiempirical method. The assumption would not usually be expected to be valid.
[17]	14	Anderson, Day, Freres, and Stokes	1.25	Not stated	6400 feet	9	The measurements were performed in Hawaii, in a region of very high rainfall. Unusual care was taken to correlate the rain gauge reading times (synchronization within ± 2 seconds is claimed), and to ensure that the rainfall intensity was uniform over the transmission path. It is stated that such periods of uniformity seldom lasted longer than 60 seconds. These appear to be among the most careful measurements recorded.
[18]	15	Rado	1.25	Not stated	2.45 miles	3	Two rain gauges were located, one at the receiver and one at the transmitter, and a third, about one-third of the way between, and nearer, the transmitter. The gauges were self-recording; the clocks of two of them are stated to be unreliable. The rainfall recorded was very nonuniform along the path. The points plotted have been reduced from the original data by a graphical process. The measurements must be regarded as very unreliable.
[15]	16	Robertson and King	1.09	Vertical	1260 feet	1	These measurements were made during two storms only. In one the rain gauge was at the transmitter. In the other it was moved to an intermediate position. The rain gauge gave average intensity over about one minute.
[19]	17	Adam, Hull, and Hurst	0.96	Not stated	2 km	1	The rain gauge was at the transmitter. It is stated that "it was possible to measure changes in intensity that lasted one minute or more." No attempt was made to ensure uniformity of precipitation intensity along the path. For such a long path, this makes the results of very doubtful accuracy.
[20]	18, 19	Okamura, Funakawa, Uda, Kato, and Oguchi	0.86	Horizontal and vertical	400 meters	1	A reflection method was used, so that the radio wave traversed the path twice. The rain gauge was read every 15, 30, or 60 seconds, depending on the rainfall intensity.
[21]	20	Okamura, Funakawa, Uda, Kato, and Oguchi	0.86	Horizontal and vertical	3.55 km	1	The same method of measurement as in [20] was used. It seems very unlikely that the precipitation intensity would often have been uniform along the path.
[22]	21	Robinson	0.86	Circular	(see "Remarks")	2	The attenuation was measured by a radar technique. Echo intensity was measured at quarter-mile intervals up to two miles, and at half-mile intervals beyond, up to a maximum of six miles. From these measurements, and with the help of the two rain gauges, one at the transmitter and one 1.75 miles away, it could be judged whether the rainfall intensity was uniform over the path. Attenuation measurements under nonuniform conditions were rejected, these occurring on about 90 percent of all occasions when rain was falling.
[23]	22	Funakawa and Kato	0.86	Not stated	24 km	3	The rain gauges were arranged one at each end and one in the middle of the path. In the figure, the abscissas are path-means, obtained by averaging 3-minute values of rain gauges along the path. It is claimed that "the rain at that time had a large rainfall area, and its variation was slow with the time."
[24]	23, 24, and 26	Usikov, German, and Vakser	0.815 0.68 0.43	Not stated	50 meters	2	A reflection method was used, as in [20]. The rain gauges were placed along the path at a distance of 30 meters from one another. Attenuation readings were used only when the rainfall intensities measured by the gauges were the same, and the intensity was not rapidly varying.
[25]	25	Mueller	0.62	Horizontal	1200 feet	1	Rain gauge at the receiving end of the path. The measured attenuations were averaged over one minute intervals, to accord with the rain gauge measurements, which were averaged over one minute.

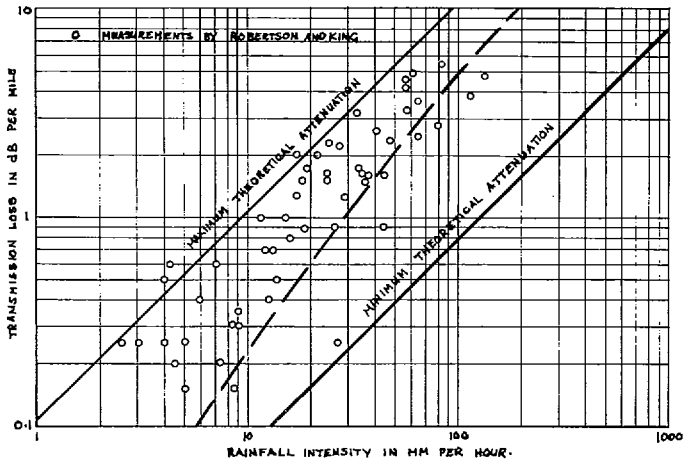

Fig. 4. Measured rainfall attenuation. $\lambda = 3.2$ cm, horizontal polarization.

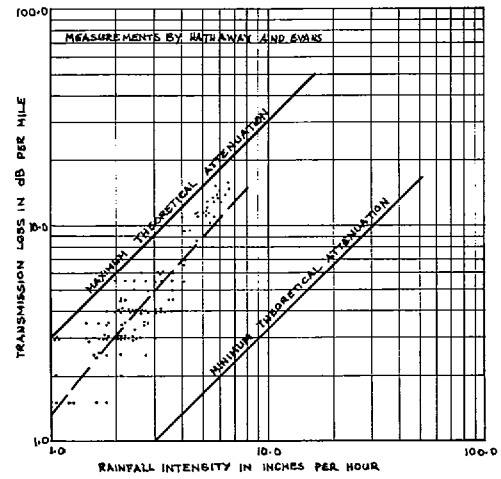

Fig. 5. Measured rainfall attenuation. $\lambda = 2.63$ cm, polarization not stated.

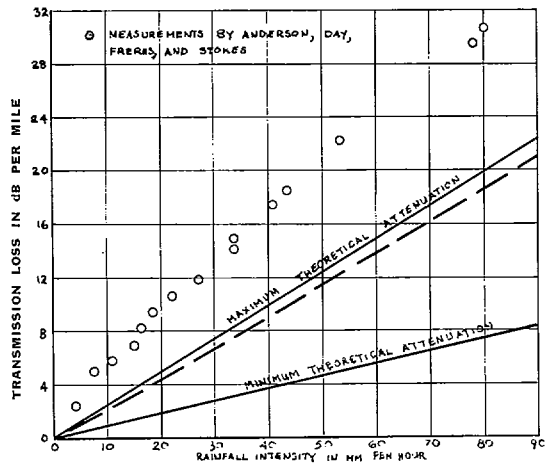

Fig. 6. Measured rainfall attenuation. $\lambda = 1.25$ cm, polarization not stated.

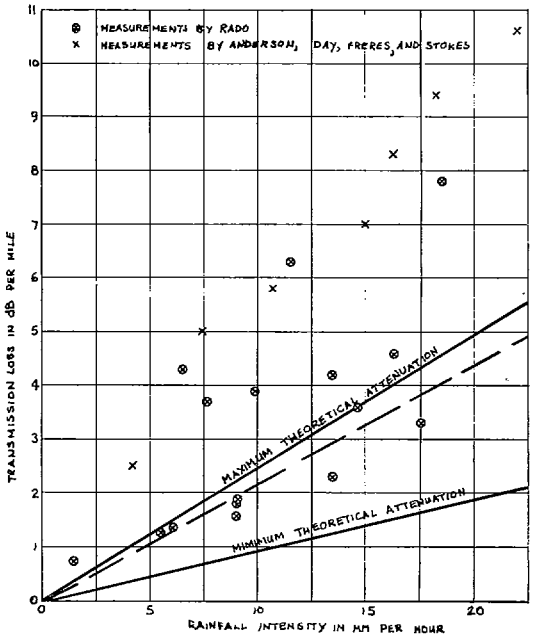

Fig. 7. Measured rainfall attenuation. $\lambda = 1.25$ cm, polarization not stated.

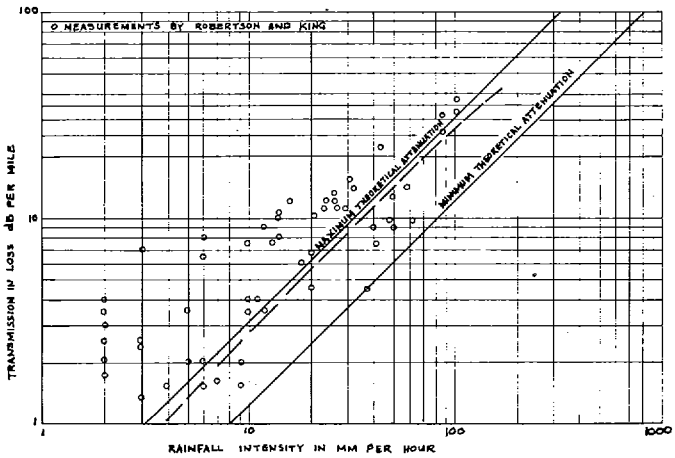

Fig. 8. Measured rainfall attenuation. $\lambda = 1.09$ cm, vertical polarization.

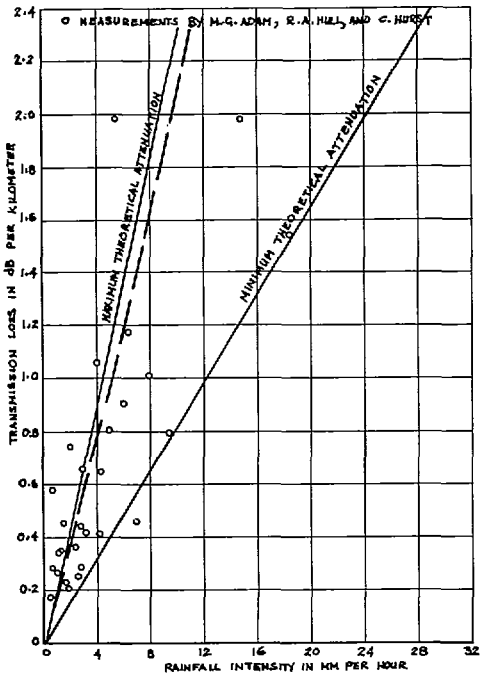

Fig. 9. Measured rainfall attenuation. $\lambda = 0.96$ cm, polarization not stated.

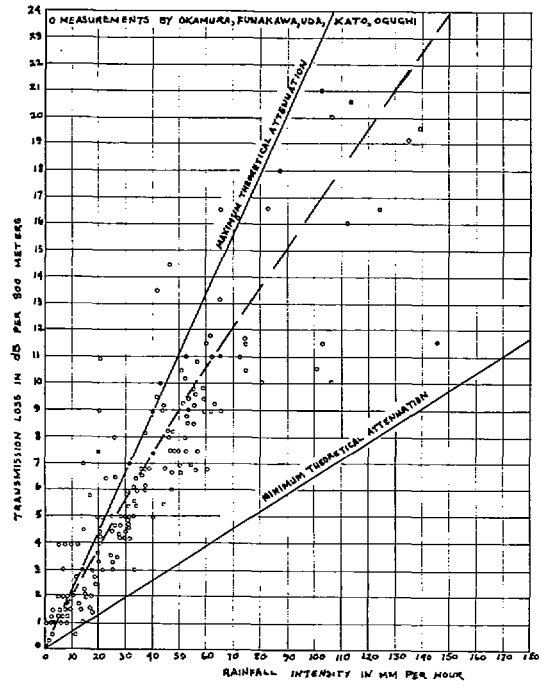

Fig. 11. Measured rainfall attenuation. $\lambda = 0.86$ cm, vertical polarization.

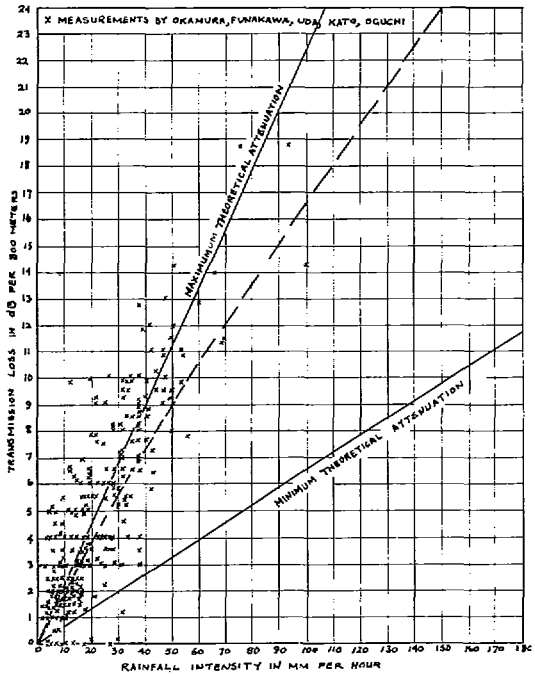

Fig. 10. Measured rainfall attenuation. $\lambda = 0.86$ cm, horizontal polarization.

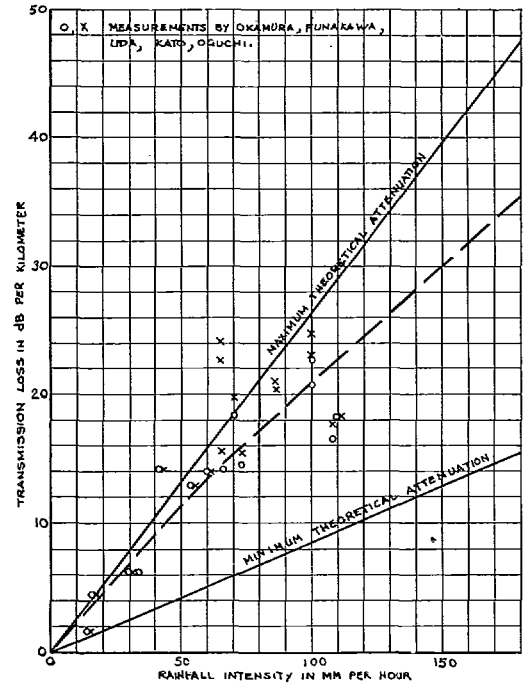

Fig. 12. Measured rainfall attenuation. $\lambda = 0.86$ cm, $\times$ horizontal polarization. O vertical polarization.

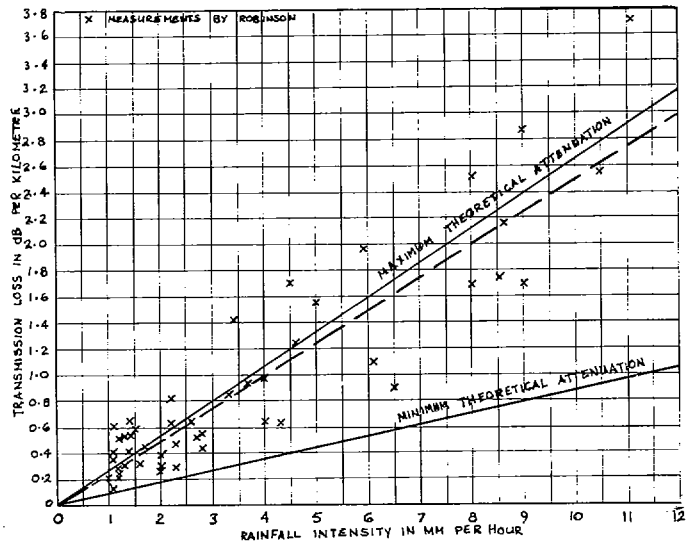

Fig. 13. Measured rainfall attenuation. $\lambda = 0.86$ cm, polarization circular.

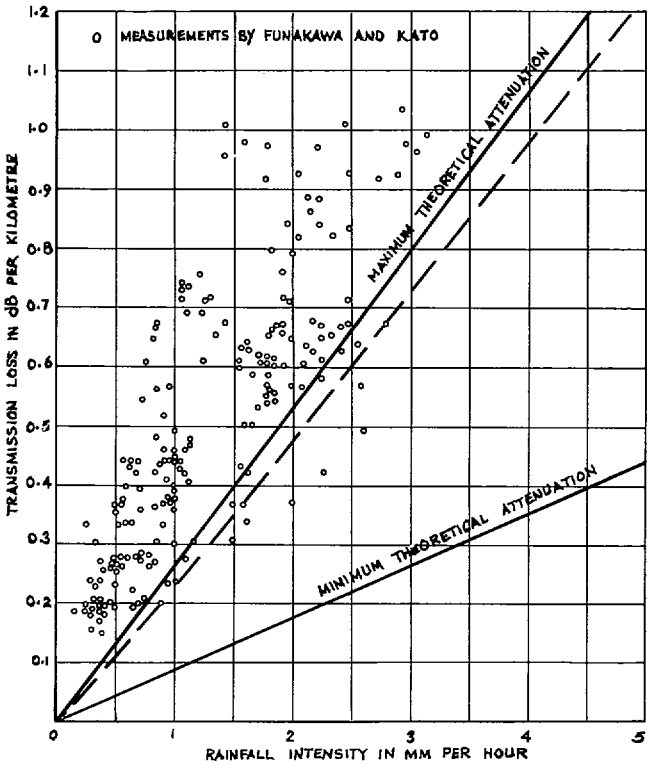

Fig. 14. Measured rainfall attenuation. $\lambda = 0.86$ cm, polarization not stated.

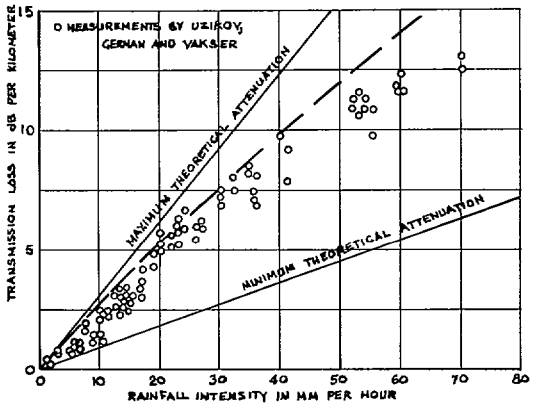

Fig. 15. Measured rainfall attenuation. $\lambda = 0.815$ cm, polarization not stated.

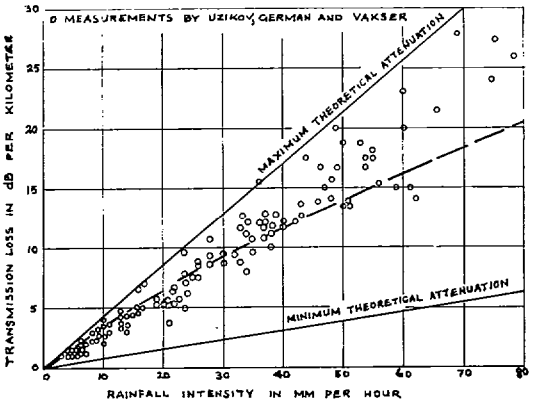

Fig. 16. Measured rainfall attenuation. $\lambda = 0.68$ cm, polarization not stated.

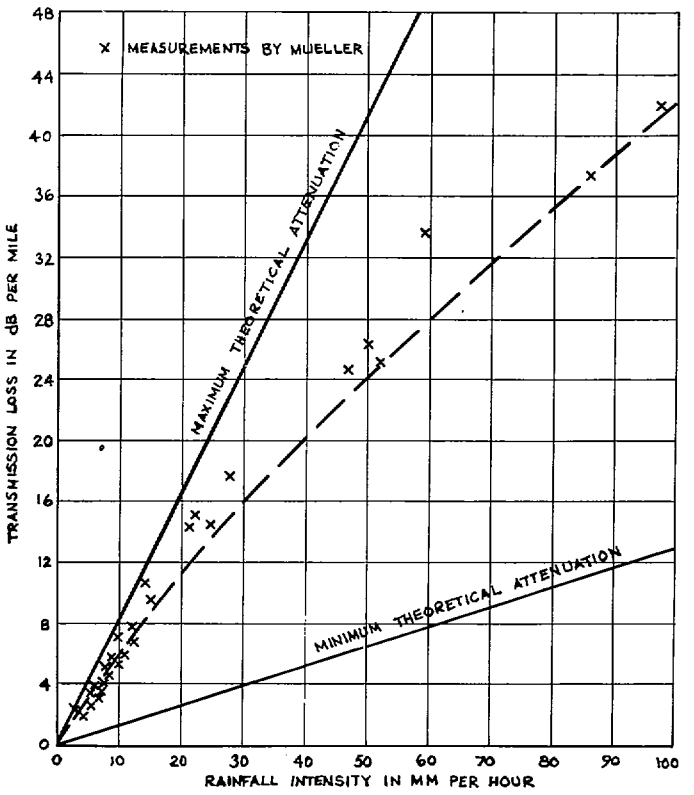

Fig. 17. Measured rainfall attenuation. $\lambda = 0.62$ cm, horizontal polarization.

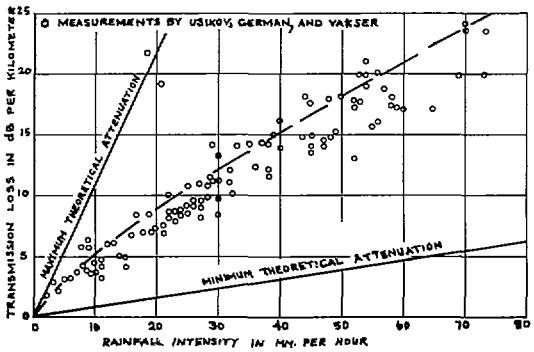

Fig. 18. Measured rainfall attenuation. $\lambda = 0.43$ cm, polarization not stated.

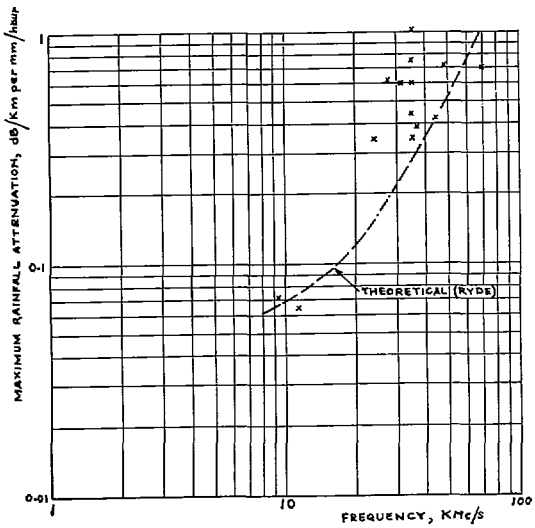

Fig. 19. Upper limit of rainfall attenuation (from measurements reported in [15]–[25]).

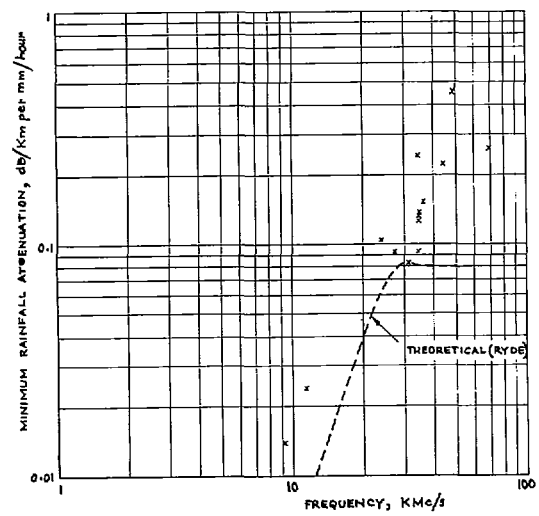

Fig. 20. Lower limit of rainfall attenuation (from measurements reported in [15]–[25]).

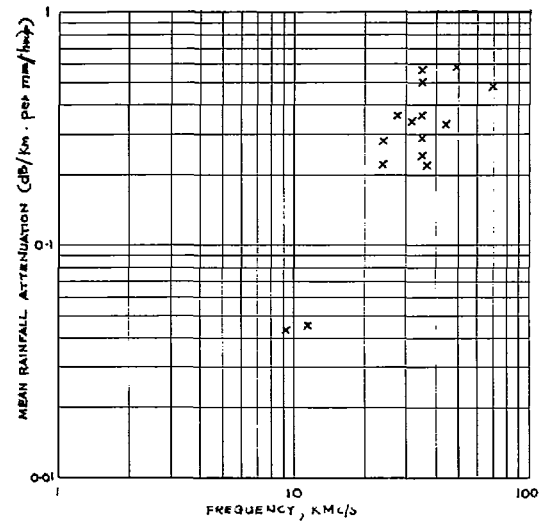

Fig. 21. Mean rainfall attenuations (from measurements reported in [15]–[25]).

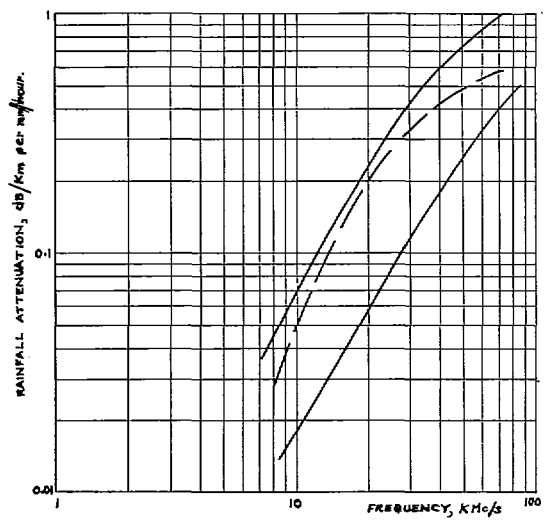

Fig. 22. Upper and lower limits and means of rainfall attenuation (from measurements reported in [15]–[25]).

VI. Conclusion

The most striking result of the present study is that while the Ryde theoretical predictions of rainfall attenuation are in qualitative agreement with measurement, the quantitative agreement is not always satisfactory. It is particularly to be noted that the maximum possible theoretical attenuation, for a given wavelength and precipitation rate, tends rather consistently to lie well below the upper range of measured attenuations.

Part of the discrepancy could be attributed to experimental error. The measurement techniques that have been used cannot, by and large, be regarded as satisfactory in a number of respects, particularly as regards the measurement of precipitation rate. One likely source of uncertainty in the measurements is the effect of wind, since it is to be expected that in the presence of wind, and particularly gusty wind, the water density in the air will be subject to variation even though the precipitation rate on the ground appears unchanged. In addition, the number of rain gauges is usually quite inadequate to ensure that measurements be made only under conditions of uniform precipitation along the path. The total attenuations observed are sometimes quite small (for example, those reported in Robertson, et al. [15] lie in the range 0.03 to 0.9 dB), and consequent measurement difficulties might account for much of the scatter shown in Figs. 4–18. It has been pointed out by one of the referees that for the lower precipitation rates part of the excess attenuation might be accounted for by the presence of fog or mist, in addition to the precipitation, though this effect should be negligible for precipitations of intensity, say, 50 mm/hour or more, where large departures from the theory have been observed.

None of these considerations seems adequate to account for the more extreme discrepancies between the theory and measurement. Attention is particularly called to the Hawaiian measurements, at $\lambda = 1.25$ cm, reported in Anderson et al. [17]. In certain important respects, these stand apart from all other rainfall attenuation measurements reported in the available literature. The density of rain gauges (nine along the 6400-foot path) is greater than has been described elsewhere, and considerable care was taken to ensure that only those measurements made under uniform rainfall conditions were taken into account. The range of measured attenuations (3 to 36 dB) is such that measurement error in the radio equipment should be small. Whether for these reasons or otherwise, the points obtained when the measured attenuations were plotted against the precipitation intensities possess the unique feature of showing virtually no scatter. They lie on a well defined curve, giving attenuation levels (in dB/mile) between $1\frac{1}{2}$ and 2 times greater than the Ryde theoretical values.

It would seem of great importance to decide whether this is a result of general validity, in which case the scatter found by other workers would have to be presumed to be due to deficiencies in experimental technique. There is clearly a need for a further series of measurements of a comparable standard, both to seek confirmation of these findings and, if they are confirmed, to extend them to cover a range of frequencies.

With the present uncertainty in the experimental situation, it is perhaps premature to try to modify the Ryde theory. However, it is as well to be aware of possible ways in which the theory may be inadequate. This author has heard it argued that Ryde's approach is so self-evidently correct that if there are discrepancies between measurements and the theory, then so much the worse for the measurements. In fact, in Ryde's theory, as in most physical theories, there are simplifying approximations, and it should not occasion undue surprise if reliable measurement did not wholly confirm the theoretical predictions.

One possible source of error consists in the neglect, in the theory, of multiple scattering effects along the path; the Ryde approach merely considers the power extracted, by absorption and scattering, from a plane wave, by an isolated drop, this "lost" power being then summed over all drops.

Another possible source of error is that the rain structure may be more complex than has been assumed. Instead of the rain consisting of drops scattered randomly through space, with average separations very much greater than the drop dimensions, evidence has recently been produced [27] suggesting that the precipitation may tend to contain clusters of two or more closely spaced drops. The findings, as published so far, are merely that the distribution with time of the number of drops in a small volume departs with statistical significance from what would be expected if clustering did not occur. It is apparently not possible to deduce from these results any quantitative information about the structure of the clusters. It is to be expected that clustering, if it occurs, could substantially modify the theory of rainfall attenuation of electromagnetic waves. Some preliminary theoretical work on these lines was carried out by Trinks [29], [30], who studied drop pairs, on the assumption that the drop diameter is much smaller than the wavelength. Further work must await elucidation of the nature of the clusters by additional meteorological observations.

References

[1] Ryde, J. W., Echo intensity and attenuation due to clouds, rain, hail, sand and duststorms at centimetre wavelengths, Rept 7831 General Electric Co. Research Labs., Wembley, England, Oct 1941.

[2] Ryde, J. W., and D. Ryde, Attenuation of centimetre waves by rain, hail and clouds, Rept 8516, General Electric Co. Research Labs., Wembley, England, Aug 1944.

[3] ——, Attenuation of centimetre and millimetre wave by rain, hail, fogs and clouds, Rept 8670, General Electric Co. Research Labs., Wembley, England, May 1945.

[4] Bussey, H. E., Microwave attenuation statistics estimated from rainfall and water vapor statistics, *Proc. IRE*, vol 38, Jul 1950, pp 781–785.

[5] Saxton, J. A., The anomalous dispersion of water at very high radio frequencies: Part II—Relation of experimental observations to theory, *1946 Conf. Rept on Meteorological factors in radio-wave propagation*, The Physical Society (London), pp 292–306.

[6] Lattey, R. T., O. Gatty, and W. G. Davies, The temperature coefficient of the dielectric constant of water, *Phil. Mag.*, vol 12, Nov 1931, pp 1019–1025.
[7] Mason, B. J., *The Physics of Clouds*. London, England: Oxford University Press, 1957.
[8] Best, A. C., Empirical formulae for the terminal velocity of water drops falling through the atmosphere, *Quart. J. R. Met. Soc.*, vol 76, Jul 1950, pp 302–311.
[9] Grunow, J., Investigations on the structure of precipitation, Final Rept to the U. S. Dept. of the Army, European Research Office, Hohenpeissenberg Meteorological Observatory, Oberbayern, Germany, Apr 1961.
[10] Laws, J. O., and D. A. Parsons, The relation of raindrop-size to intensity, *Trans. Am. Geophysical Union*, vol 24, 1943, pp 432–460.
[11] Al'pert, Ya. L., *Radio Wave Propagation and the Ionosphere*. New York: Consultants' Bureau, 1963.
[12] Aden, A. L., Electro-magnetic scattering from spheres with sizes comparable to the wavelength, *J. Appl. Phys.*, vol 22, May 1951, pp 601–605.
[13] Oguchi, T., Attenuation of electro-magnetic wave due to rain with distorted raindrops, *J. Radio Research Labs. (Tokyo)*, vol 7, Sep 1960, pp 467–485.
[14] Wolff, I., and E. G. Linder, Transmission of 9 cm electro-magnetic waves, *Broadcast News*, no 18, Dec 1935, pp 10–13.
[15] Robertson, S. D., and A. P. King, The effect of rain upon the propagation of waves in the 1- and 3-centimeter regions, *Proc. IRE*, vol 34, Apr 1946, pp 178P–180P.
[16] Hathaway, S. D., and H. W. Evans, Radio attenuation at 11 kmc and implications affecting relay system engineering, *Bell Sys. Tech. J.*, vol 38, Jan 1959, pp 73–98.
[17] Anderson, L. J., J. P. Day, C. H. Freres, and A. P. D. Stokes, Attenuation of 1.25-centimeter radiation through rain, *Proc. IRE*, vol 35, Apr 1947, pp 351–354.
[18] Rado, G. T., Measurements of the attenuation of K-band waves by rain, Rept 603, Radiation Lab., Massachusetts Institute of Tech., Cambridge, Mar 1945.
[19] Adam, M. G., R. A. Hull, and C. Hurst, Absorption of 1 cm radiation by rain, Rept C. L. Misc. 3, C.V.D. Research Group, New Clarendon Lab., Oxford, England, Jun 1942.
[20] Okamura, S., K. Funakawa, H. Uda, J. Kato, and T. Oguchi, On the measurement of attenuation by rain at 8.6 mm wave length, *J. Radio Research Labs. (Tokyo)*, vol 6, Apr 1959, pp 255–267.
[21] ——, Effect of polarization on the attenuation by rain at millimeter wave length, *J. Radio Research Labs. (Tokyo)*, vol 8, Mar 1961, pp 73–80.
[22] Robinson, N. P., Measurements of the effect of rain, snow and fogs on 8.6 mm radar echoes. *Proc. IEE*, vol 102, pt B, Sep 1955, pp 709–714.
[23] Funakawa, K. and J. Kato, Experimental studies of propagation characters of 8.6 mm wave on the 24 km path, *J. Radio Research Labs. (Tokyo)*, vol 9, Sep 1962, pp 351–367.
[24] Usikov, O. Ya, V. L. German, and I. Kh. Vakser, Investigation of the absorption and scatter of millimeter waves in precipitations, *Ukr. Fiz. Zh.*, vol 6, 1961, pp 618–540.
[25] Mueller, G. E., Propagation of 6-millimeter waves, *Proc. IRE*, vol 34, Apr 1946, pp 181P–183P.
[26] Mie, G., Beitrüge zur Optik trüber Medien, speziell kolloidaler Metallosungen, *Ann. der Phys.*, vol 25, Mar 1908, pp 377–445.
[27] Dingle, A. N., The micro-structure of rain in a summer shower, *Proc. Eighth Weather Radar Conf.*, 1960, pp 99–106.
[28] Stratton, J. A., *Electromagnetic Theory*. New York: McGraw-Hill, 1941, pp 563–573.
[29] Trinks, W., Zur Vielfachstreuung an kleinen Kugeln, *Ann. der Phys.*, vol 22, Apr 1935, pp 561–590.
[30] Lillesaeter, O., Scattering of microwaves by adjacent water droplets in air, *Nature*, vol 202, Jun 13, 1964, pp 1103–1104.

An Analysis of the Effects of Ground Reflection in Line-of-Sight Phase Systems

MOODY C. THOMPSON, JR., SENIOR MEMBER, IEEE

Abstract—**The presence of a reflected component in a line-of-sight radio system influences the phase variability resulting from atmospheric changes along and near the path. An analysis is made of a simple case showing the general nature of this effect and the parameters upon which it depends. A method is presented for calculating the phase behavior of the resultant signal, in terms of that expected from a single direct component, and the relevant system parameters.**

INTRODUCTION

THE PHASE BEHAVIOR of a radio wave, after propagation over a line-of-sight path which includes a single quasi-specular reflection mechanism, is influenced by the reflection mechanism. The resultant phase is determined, not only by the atmospheric index along the line-of-sight path, but also by the index along the ground-reflection path. Furthermore, the characteristics of this additional path enter in a nonlinear way which varies in importance depending on the nominal phase shift resulting from the excess path length of the reflected ray. The latter is determined by the radio wavelength, antenna-reflector geometry, and the properties of the reflector. Since in various applications adjustment of one or more of these factors may be practical, it is important to understand their relationship.

Utilization of highly directive antennas can reduce these reflection effects by reducing the amplitude of the reflected component relative to the direct ray. Even so, it is desirable to further reduce the minimum elevation angle at which phase systems may be operated. For elevation angles less than the half-beamwidth of the antenna, the ground ray cannot be neglected. In fact, the sidelobe structure of the antenna pattern may make the reflection mechanism important some time before the dimension of the main lobe is reached.

There are various configurations in which this phenomenon may play an important role. Ground-to-

Manuscript received December 31, 1964; revised March 1, 1965.
The author is with the Central Radio Propagation Lab., Boulder Labs., National Bureau of Standards, Boulder, Colo.